Cr(VI) and Cu(II) adsorption from aqueous medium using eucalyptus wood waste derived biochar

Yu Shuang Ren[a], Saeeda Yousaf[b], Muhammad Ilyas[b,c,]*, Sara Bibi[c]

[a]*School of Economics and Management, Jilin Jianzhu University, Chang Chun 130117, China, email: rysmiracle@126.com (Y.S. Ren)*
[b]*Department of Environmental Sciences, University of Peshawar, Peshawar, Khyber Pakhtunkhwa, Pakistan, Tel. +923078064028; emails: sirfilyas@yahoo.com (M. Ilyas), saeeda@uop.edu.pk (S. Yousaf)*
[c]*Department of Environmental Sciences, Shaheed Benazir Bhutto University Wari Campus, Dir Upper, Khyber Pakhtunkhwa, Pakistan, email: girlpakistani03@gmail.com (S. Bibi)*

ABSTRACT

The current study reports batch studies using eucalyptus wood waste derived biochar (EWB) to adsorb Cr(VI) and Cu(II) from aqueous solutions. Scanning electron microscopy, specific surface analysis, and Fourier-transform infrared spectroscopy were used to study the morphology and structure of the EWB. A thorough analysis of the variables affecting adsorption performance was conducted. The Freundlich isotherm, Langmuir isotherm, pseudo-second-order, and pseudo-first-order models were used to study the adsorption process. The optimal conditions for the highest adsorption of Cr(VI) and Cu(II) as of aqueous solution on the EWB adsorbents were found to be an initial concentration of 30 ppm, contact time of 60 min, temperature of 60°C, adsorbent dose of 0.20 g, and 3, 6 pH. The adsorption system, according to kinetic studies, follows a pseudo-second-order equation. It was shown that the experimental results for the adsorption of Cr(VI) and Cu(II) on EWB were best suited by the Langmuir equation. The trial results revealed that the highest adsorption at optimum condition for Cr(VI) and Cu(II) from aqueous medium was 96.23% and 98.46%, respectively. The produced EWB have a high adsorption capacity (>95%) and a porous structure that make them very attractive as an alternative to Cr(VI) and Cu(II) adsorbents.

Keywords: Biochar; Metal adsorption; Aqueous medium; Kinetic and isotherm

1. Introduction

One of the most significant issues we currently have is the management of industrial wastewater. Industrialization, highly urbanized cultures, and rising population density are to blame for this [1]. Water contamination is accelerated by increased urbanization and industry, which release heavy metals (HMs) into the environment [2]. The metals with specific gravities larger than 5.0 and atomic weights between 63.5 and 200.6 are referred to as HMs [3]. HMs in wastewater cannot be destroyed like organic contaminants, hence they persist in wastewater [1,2]. HMs build up in the food chain, disrupting the environment and perhaps endangering human health. Humans are exposed to HMs and other hazardous compounds through contaminated food, water, and air. Human bioaccumulation has been seen to be caused by HM concentrations [4].

Given their frequent occurrence in wastewater, it is imperative to remove HMs like Cu(II) as well as Cr(VI) as of aqueous solutions in order to employ these metal ions in a variety of industries, including chemical production, mining, tanning, and metal plating [5]. Complexation, chemical precipitation, electrochemical treatment, filtration, membrane technology, coagulation or flocculation, chemical

---

* Corresponding author.

reduction/oxidation, biosorption, and chemical precipitation are common methods for removing HMs from wastewater [6]. These tactics are difficult, costly, ineffective, and time-consuming [7]. However, each invention has unique challenges, such as the development of hazardous sludge, intermediate harmful chemical production, greater costs associated with high energy requirements, and incomplete removal [1].

Toxic metals can be removed from wastewater using the effective wastewater treatment method known as adsorption [1]. A variety of adsorbents utilized for this reason incorporates chemically treated biosorbents [8,9], polyacrylonitrile/Na-Y-zeolite composite [10], biochar/bentonite/waste polyethylene terephthalate as well as biochar/bentonite/waste polystyrene [1], *Phoenix dactylifera* coir wastes [11], magnetic chitosan grafted with Schiff's base polymer [12], L-cystein-modified montmorillonite-immobilized alginate nanocomposite [13], microalgae [14], synthetic chelating resin [15], poly(methyl methacrylate)-grafted alginate/Fe_3O_4 nanocomposite [16], various other adsorbents [17], biosorbents [18], montmorillonite clay [19], ligand embedded nano-conjugate adsorbent [20], greenly synthesized nanoengineered materials [21], green synthesis of silver nanoparticles [22], ligand based composite material [23], metal/mineral-incorporating materials [24], iron oxide-impregnated dextrin nanocomposite [25], ether based mesoporous adsorbent [26], magnetic glycine-modified chitosan [27], papaya peel carbon [28], ligand functionalized organic–inorganic based novel composite [29], thiourea-formaldehyde resin and its magnetic derivative [30], chitosan grafted polyaniline [31], modified conjugate material [32], CuO and $Cu(OH)_2$ embedded chitosan [33], waste rubber tires [34], ligand doped conjugate adsorbent [35], magnetic glycidyl methacrylate resin [36], iron based metal organic framework [37], novel optical adsorbent [38], ligand based efficient conjugate nanomaterials [39], novel facial composite adsorbent [40,41], cockle shell waste [42], wastepaper [43], a tamarind seeds activated carbon [44] and coconut shell activated carbon [45]. Further research has shown that biochar may remove several organic contaminants and metals from the environment [46].

In the present investigation, the eucalyptus wood waste derived biochar (EWB) has been prepared successfully by a simple and low-cost method. Investigations were conducted on the structural characteristics of the EWB as well as the adsorption states of Cr(VI) and Cu(II). Through batch studies, the effectiveness of EWB adsorption was assessed, and its adsorption behaviour for Cr(VI) and Cu(II) was carefully examined, including the effect of initial Cr(VI) and Cu(II) concentration, temperature, contact time, pH, adsorbent dose, adsorption isotherm, and adsorption kinetics. This study makes a significant contribution to the removal of hazardous Cr(VI) and Cu(II) from wastewater and establishes a new benchmark for lowering environmental pollution by reducing solid waste and plastic debris. This in turn raises the local environment aesthetic value.

2. Materials and methods

In the current study, waste eucalyptus wood was turned into biochar, which was then used as an adsorbent to remove toxic metals like Cr(VI) and Cu(II) from aqueous solutions. The following methodology was adopted for achieving the above-mentioned objective.

2.1. Chemicals and materials

Biochar manufactured from eucalyptus wood waste was supplied by the University of Agriculture (Peshawar, Pakistan). Water used in this investigation was deionized, and all utilized substances and solvents were highly pure and used without additional purification. Making stock solutions of copper(II) sulphate ($CuSO_4$) and potassium dichromate ($K_2Cr_2O_7$) in distal water yield 1,000 mg·L^{-1} of Cr(VI) and Cu(II) correspondingly. Reagent grade ingredients were also used, including HCl and NaOH.

2.2. Preparation of EWB

Pyrolysis at 450°C for 1 h in a high-performance, automatically controlled furnace with a continuous flow of nitrogen was the procedure used to produce biochar from eucalyptus wood waste. The heavy tar was condensed by passing the exhaust through a cooling chamber with water. The EWB were subsequently cooled to room temperature in a furnace while being exposed to nitrogen.

2.3. Characterization

The JSM-5910 (JEOL, Japan) scanning electron microscopy (SEM) instrument was used to carry out the EWB SEM examination. A Nicolet iS10 FTIR spectrometer (Cary 630, Agilent Technologies, USA) with a scanning range of 4,000–400 cm^{-1} was used to measure the Fourier-transform infrared (FTIR) spectra. The average pore size, total pore volume, and specific surface area were calculated using a Quantachrome, USA, model NOVA 2200e porosimetry system and surface area. All experiments were performed using the laboratory facilities of the Department of Environmental Sciences, Central Resource Laboratory (CRL) and Institute of Chemical Sciences, University of Peshawar (Pakistan).

2.4. Adsorption experiments

Adsorption research has been done using the batch equilibrium approach. The analyses were carried out by varying the EWB concentrations (5%, 10%, 15%, and 20%) and the contact periods (15, 30, 45, and 60 min) in a single metal solution while keeping the pH between 1 and 7. To achieve the ideal pH, we use 0.1 M NaOH or HCl. At room temperature, mix the mixture for various contact periods at 200 rpm. At this point, filtering was used to separate the liquid from the EWB. An atomic absorption spectrophotometer (AAnalyst 700, PerkinElmer, USA) equipped with an HGA graphite furnace was used for the filtrate analysis.

2.5. Mathematical modelling

Before applying a kinetic or isotherm model, it is necessary to find the adsorption equilibrium concentration experimentally and determine the adsorption capacity using Eq. (1) [1].

$$q_e = \frac{\left[(C_o - C_i)V \right]}{m} \tag{1}$$

where C_i and C_o are the final and initial concentrations (in mg·L^{-1}, respectively), and q_e (mg·g^{-1}) denotes the concentration adsorbed on the EWB. V stands for the aqueous solution volume (L) and m for the adsorbent mass (g). Only the average values of the three triplicates are shown for all tests.

To calculate the percentage of Cr(VI) and Cu(II) ions removed (%MR), Eq. (2) was utilized.

$$\%\text{MR} = \frac{\left[(C_o - C_i) \times 100 \right]}{C_o} \tag{2}$$

2.6. Isotherm modelling

The Langmuir isotherm in linearized form [1]:

$$\frac{C_e}{q_e} = \frac{1}{KQ} + \frac{C_e}{Q} \tag{3}$$

The Freundlich isotherm in linearized form [1]:

$$\ln q_e = \ln K_f + \frac{1}{n}\ln C_e \tag{4}$$

where q_e stands for the concentration adsorbed on the EWB (mg·g^{-1}), C_e for the metal ions equilibrium concentration (mg·L^{-1}), and n and K_f for the model constant and adsorption coefficient, respectively.

2.7. Kinetics modelling

The adsorption capacity should be determined using the aforementioned equation before employing various kinetic models at various times. pseudo-first-order and pseudo-second-order kinetic models are the most widely used types. The pseudo-first-order kinetic rate law is given in Eq. (5) [1]:

$$\ln(q_e - q_t) = \ln q_e - k_1 t \tag{5}$$

where q_e (mg·g^{-1}) represents the amount of metal ions adsorbed at equilibrium, q_t (mg·g^{-1}) represents the amount of metal ions adsorbed at time t, and k_1 (min^{-1}) represents the rate constant. By plotting $\ln(q_e - q_t)$ vs. t, it is possible to determine k_2 and q_e from the slope and intercept, respectively.

Eq. (6) represents the pseudo-second-order kinetic rate law [1]:

$$\frac{t}{q_t} = \frac{t}{q_t} + \frac{1}{k_2 q_e^2} \tag{6}$$

where q_e gives the sorption capacity at equilibrium and k_2 is the rate constant (g·mg^{-1}·min^{-1}) for second-order kinetics. Plotting t/q_t vs. t yields q_e and k_2, which may be derived from the slope and intercept, respectively.

3. Results and discussion

3.1. Characterization analysis

SEM, FTIR, and surface area analysis were used to characterize EWB prepared in the laboratory. Fig. 1a shows that the EWB is flattened like a sponge. On the surface, it showed bigger spicules and agglomeration development. Fig. 1b shows the surface of EWB after adsorption of Cr(VI) and Cu(II), which becomes shiny and smooth with a closed pore structure, probably as a result of the physico-chemical interaction between the functional groups on the EWB surface and the Cr(VI) and Cu(II).

The FTIR spectrum of the EWB sample (Fig. 2) shows peaks centered around 3,000 and 2,800 cm^{-1}, corresponding to aromatic C–H and methylene C–H bonds. Multiple peaks at 1,630 and 1,500 cm^{-1} represent aromatic C=C, and peaks around 1,447 cm^{-1} and 693 represent methylene C–H vibrations.

The pore size, pore volume, Brunauer–Emmett–Teller surface area (S_{BET}), and Barrett–Joyner–Halenda surface area (S_{BJH}) of the EWB were all calculated using the N$_2$ adsorption isotherm at 77.35 K (Fig. 3). The survey findings are listed in Table 1. Based on the surface analysis results (Table 1), the calculated S_{BJH} of the EWB was 14.10 m^2·g^{-1}. The S_{BET} was found to be 18.37 m^2·g^{-1}, the pore volume was 0.01 cm^3·g^{-1}, and the pore radius was 14.90 A^0. The statistics demonstrate that the EWB adsorbent has a large pore size and a high surface area. Therefore, EWB has
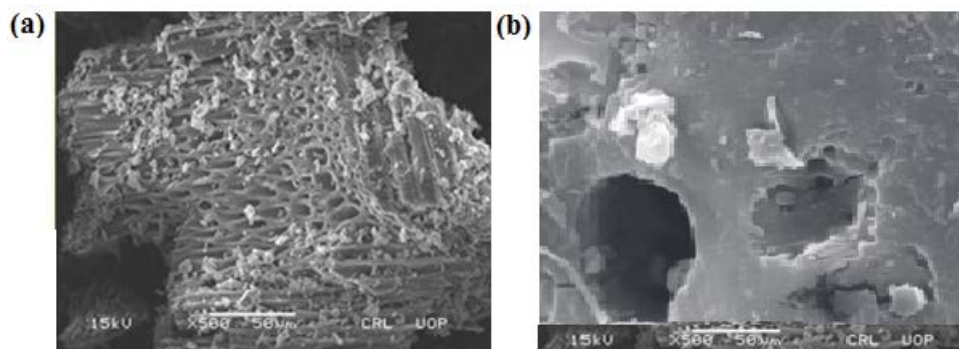

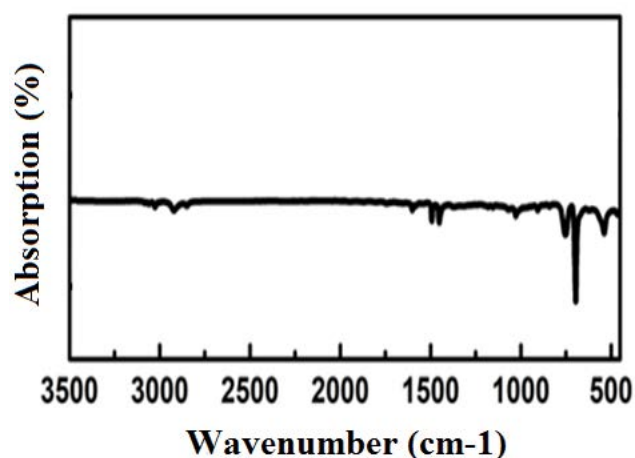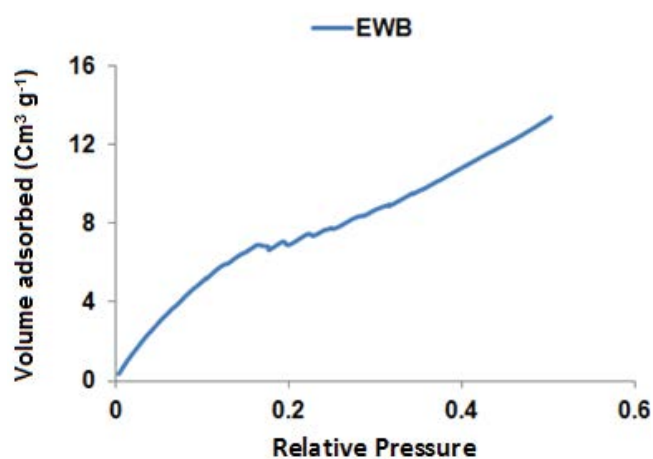Fig. 1. Scanning electron microscopy images of EWB (a) before and (b) after adsorption.

Fig. 2. Fourier-transform infrared spectra of EWB.

Fig. 3. N$_2$ adsorption isotherms of EWB at 77 K.

Table 1
Surface properties of the EWB

Adsorbent	S_{BJH} (m$^2 \cdot$g^{-1})	S_{BET} (m$^2 \cdot$g^{-1})	Pore radius (A^0)	Pore volume (cm$^3 \cdot$g^{-1})
EWB (Before adsorption)	14.10	18.37	14.90	0.01
EWB (After adsorption)	1.99	2.12	3.28	0.0001

better adsorption potential. The surface characteristics were seen to decrease after adsorption, which confirmed the adsorption of Cr(VI) and Cu(II).

3.2. Effects of the studied parameters on the adsorption capacity

The initial adsorption studies were carried out under constant conditions, for instance, with an EWB adsorbent to solution ratio of 0.10 g/20 mL, temperature of 24°C ± 2°C, stirring speed (100 rpm) and contact time (40 min). After
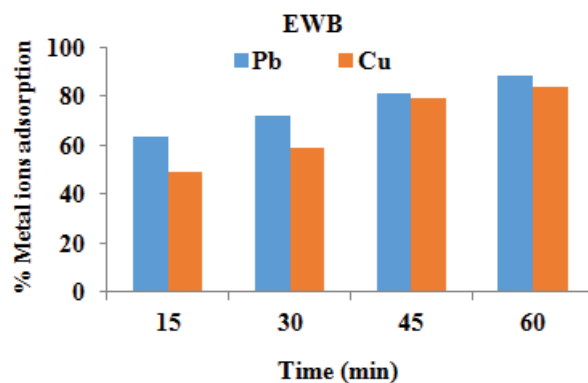

Fig. 4. Effect of contact time on adsorption of Cr(VI) and Cu(II) on EWB.

looking at EWB efficiency, it was found that it had higher adsorption efficiency. To identify the optimal conditions required for the maximum adsorption of Cr(VI) and Cu(II), adsorption was investigated under a variety of contact duration, adsorbent dose, temperature, concentration of Cr(VI) and Cu(II), and pH conditions.

3.2.1. Effect of contact time

Studying the effects of different contact time intervals (15, 30, 45, and 60 min) on the adsorption of Cr(VI) and Cu(II) ions from aqueous solutions. The results showed that the % adsorption increases with increasing contact time. Higher adsorption with longer contact times is caused by the availability of Cr(VI) and Cu(II) ions to adsorb on the EWB surface. In the current trial conditions, the maximum percent adsorption of 96.26 and 94.58 for Cr(VI) and Cu(II) ions, respectively, from aqueous medium was achieved (Fig. 4). In earlier studies on metal ions adsorption over a variety of adsorbents, similar results that the adsorption of metal ions increases as the adsorption period increases and approaches equilibrium have also been reported [47].

3.2.2. Effect of adsorbent dose

The amount of utilized adsorbent represents the accessibility and availability of adsorption sites [1]. Additionally, the adsorption of Cr(VI) as well as Cu(II) ions by EWB at different adsorbent dosages (5%, 10%, 15%, and 20%) was investigated. The findings showed that the % adsorption increases with increasing adsorbent dosage. At a 20% adsorbent dose, the maximum percent adsorption for Cr(VI) and Cu(II) ions, respectively, was noted as shown in Fig. 5. Moreover, the adsorption that followed this stage tended to become more consistently steady. Adsorption sites and available adsorbent surface area may have increased in response to the increase in percent expulsion of metal ions that resulted from increasing adsorbent dosages. Since then, despite further increases in adsorbent measurement, no critical reduction in adsorption efficacy has been seen, which may be due to an accumulation of adsorbent particles that covers up the adsorption sites. Similar behaviour has been observed in earlier studies and results from the interaction of adsorbent and metal ion interactions.
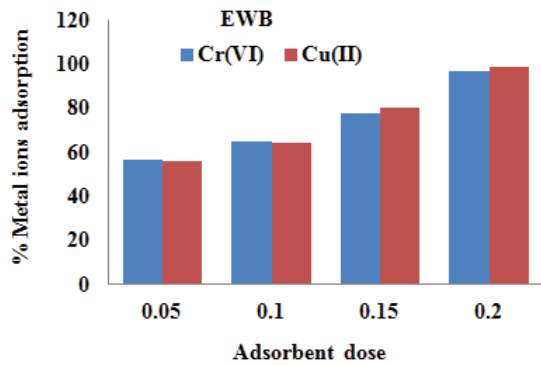
Fig. 5. Effect of adsorbent dose on adsorption of Cr(VI) and Cu(II) on EWB.
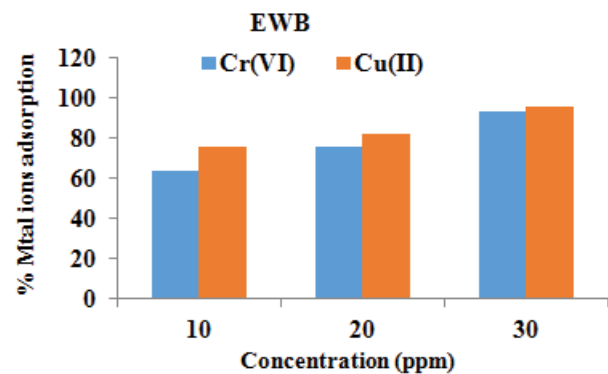

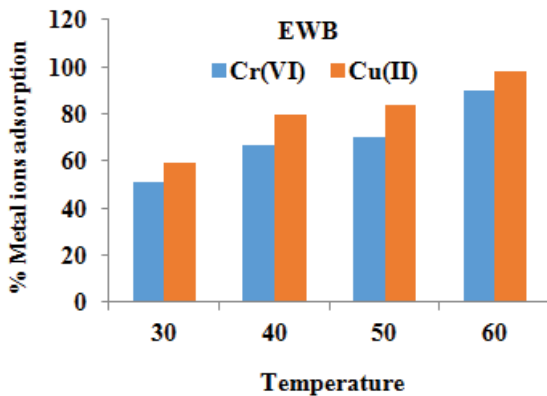Fig. 7. Effect of initial concentration on adsorption of Cr(VI) and Cu(II) on EWB.

Fig. 6. Effect of temperature on adsorption of Cr(VI) and Cu(II) on EWB.

Fig. 8. Effect of pH on adsorption of Cr(VI) and Cu(II) on EWB.

The large number of adsorption sites and surface area are consistent with the enhanced dose [48].

3.2.3. Effect of temperature

Fig. 6 illustrates how temperature (30°C, 40°C, 50°C, and 60°C) affects the percentage of Cr(VI) and Cu(II) that is adsorbed from an aqueous solution. The adsorption capacity rises as the temperature rises. That is comparable to how the reaction rate increases as temperature does. The surface becomes activated, and the capacity for adsorption rises. The favorable intermolecular forces between the adsorbate and the adsorbent in this situation are substantially stronger as the temperature rises than those between the adsorbate and the solvent. Adsorbate becomes easier to adsorb as a result of the temperature rising. For Cr(VI) and Cu(II), the maximum % adsorption capacity of EWB was 97.28% and 96.14%, respectively. Additionally, the rising temperature indicates an increased probability of adsorption at higher temperatures, which is consistent with a previous finding [49].

3.2.4. Effect of initial metal ion concentration

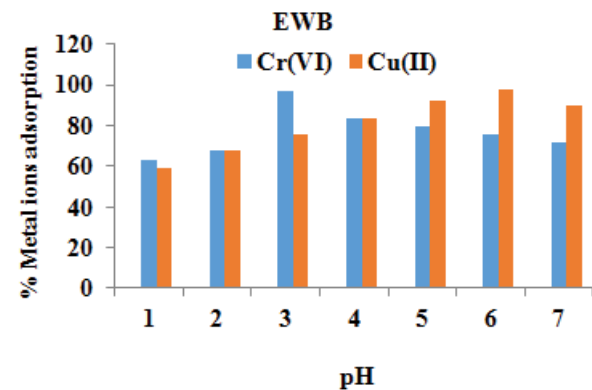Fig. 7 shows that as the initial metal concentration increased, more metals were adsorbed onto the EWB. This is due to the possibility that increasing the initial metal concentration will make more metal ions available to adsorb over the active EWB composite surface sites. It is possible to hypothesise that a greater initial concentration of Cr(VI) and Cu(II) will facilitate the adsorption process because the initial concentration acts as a crucial driving factor to overcome the mass transfer resistance of metal ions between the aqueous and solid phases [1].

3.2.5. Effect of pH

The influence of pH on Cr(VI) and Cu(II) on EWB was examined in the pH range of 1–7 (Fig. 8), as pH is a significant characteristic of the solution that affects the adsorbent water interface for metal ion adsorption. As metal hydroxide precipitation may occur when the pH exceeds 7, experiments on the influence of pH were conducted in neutral and acidic single metal solutions. The highest percentage of Cr(VI) adsorption capacity recorded with EWB at pH 3 was 96.62%, respectively. While the greatest percentage adsorption capacity for Cu(II) at pH 6 was found to be 97.64%. It was obvious from the data that the % adsorption capacity increases with an increase in pH from 1–6, after a decreasing trend in % adsorption capacity were noted for Cu(II) at pH 7 using the EWB. The % adsorption capacity of EWB for Cu(II) is reduced at low pH as a result of competition between H+ and Cu(II) ions for the adsorbent negatively charged sites in the solution.

3.3. Kinetic study

The adsorption behaviour of EWB during Cr(VI) and Cu(II) adsorption from the solution was studied by applying the kinetic model Fig. 9a and b. The adsorption affinity of EWB toward Cr(VI) and Cu(II) was high. The outcomes of the examinations are shown in Table 2.

A very high value of coefficient of determination for Cr(VI) and Cu(II) in the pseudo-second-order model was found. In the case of Cr(VI) the adsorption potential and adsorption coefficient were observed to be 0.097 and 2.1×10^{-4} mg·g^{-1}, respectively, for the second-order model, whereas, the calculated value of the adsorption potential and adsorption coefficient was found to be 0.568 and 53.428 mg·g^{-1}, respectively for Cu(II). In spite of the fact that the coefficient of determination for the pseudo-second-order model was the highest, showing that the adsorption system follows a pseudo-second-order kinetics. Several authors have also reported the applicability of the pseudo-second-order kinetic model for other sorbents [49–51]. According to the pseudo-second-order model [1], it is generally assumed that the adsorption of Cr(VI) and Cu(II) onto EWB is a chemisorption in which valence forces are generated through the contribution or exchange of electrons between the adsorbent and the adsorbate.

3.4. Isotherm study

The equilibrium adsorption data were evaluated using the Freundlich and Langmuir isotherms. Table 3 lists the parameters for the Langmuir isotherms that were computed from the experimental data for the Cr(VI) and Cu(II) adsorption isotherm models.

The results of fitting experimental data to the Langmuir isotherms for Cr(VI) and Cu(II) are shown in Fig. 10a and b. The Cr(VI) and Cu(II) adsorption on EWB follows the Langmuir isotherm, as shown by the straight line plots of the Langmuir isotherm model. The fact that the Cr(VI) and Cu(II) adsorption data gave a superior match in the Langmuir isotherm model is shown by the greater estimation of R^2 (correlation coefficient) for Langmuir than for Freundlich isotherm, which were firmly identified with Langmuir model parameters in other studies [5]. The Langmuir hypothesis postulates that during the process, the adsorbate will cover homogeneous and equivalent sites on the adsorbent in a monolayer [1].

3.5. Industrial wastewater treatment

Management of industrial and municipal wastewater has become an inevitable challenge in the modern-day world, because of the extensive industrialization and rapid growth in human population around the world [1]. Heavy environmental contamination is brought on by excessive urbanization, which is linked to a high consumption of products made in factories that contain both trace and heavy metals in varying concentrations [2]. Diverse harmful metals make their way into water bodies, where they enter the food chain and a pose serious health risks to human. Different toxic metals have been reported to cause different physiological toxicities, but in general, trace and heavy metals are known to be associated with damage of nerves, kidney, liver, bones, and block the enzyme functional groups [2]. As a result of their constant presence in wastewater, the removal of toxic metal ions is essential.

Toxic metals can be removed and recovered from our environment and wastewater using a variety of physical and chemical techniques. The removal of Cu(II) and Cr(VI) from wastewater using EWB adsorbent was studied utilizing the batch adsorption test. The experimental findings demonstrate that the maximum adsorption rates of Cr(VI) and Cu(II) for EWB under the optimum circumstances (30 ppm concentration, 0.20 g adsorbent dosage, 60 min contact time, temperature 60°C, and 3.6 pH) were 98.2% and 98.6%, respectively.

3.6. Comparison of adsorption potential of different adsorbents

Table 4 compares the adsorption efficiencies of the adsorbents (particularly EWB and various adsorption
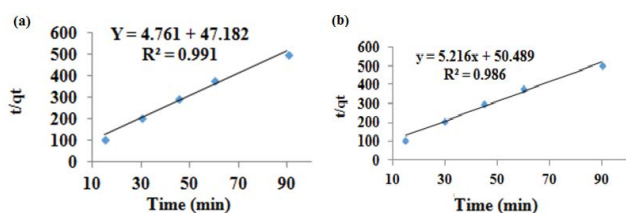

Fig. 9. Pseudo-second-order kinetics for the adsorption of (a) Cr(VI) and (b) Cu(II) onto EWB.

Table 2
Pseudo-second-order kinetic parameters for adsorption of Cr(VI) and Cu(II) over EWB adsorbents

	Cr(VI)	Cu(II)
k_2 (mg·g^{-1}·min^{-1})	0.001	0.192
q_{e2} (mg·g^{-1})	0.210	0.568
R^2	0.991	0.986

Table 3
Langmuir isotherm parameters for Cr(VI) and Cu(II) adsorption

	Cr(VI)	Cu(II)
q_m (mg·g^{-1})	0.164	0.141
k_1	0.395	0.673
R^2	0.989	0.989

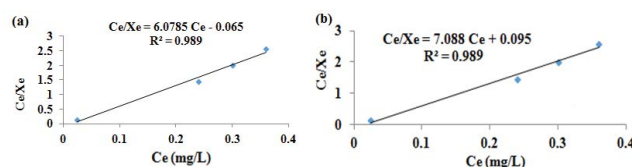Fig. 10. Langmuir isotherms for (a) Cr(VI) and (b) Cu(II) onto EWB.

Table 4
Comparison of different adsorbents used for Cr(VI) and Cu(II) adsorption

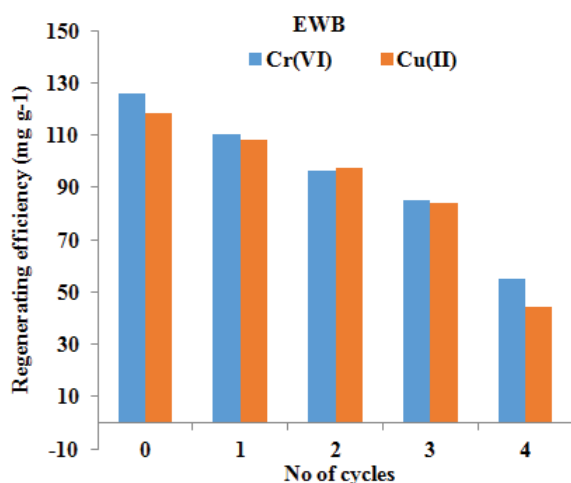| Adsorbent	Adsorption potential		References
	Cr(VI)	Cu(II)	
Polyaniline/paly-gorskite composite	198 mg·g^{-1}	114 mg·g^{-1}	[52]
Polyaniline	101 mg·g^{-1}	92 mg·g^{-1}	[52]
Activated carbon	34.70 mg·g^{-1}	24.21 mg·g^{-1}	[53]
Expanded perlite	–	8.62 mg·g^{-1}	[54]
Acid activated palygorskite	–	32.24 mg·g^{-1}	[55]
Cross-link cationic starch	97.08 mg·g^{-1}	–	[56]
Palygorskite	30.70 mg·g^{-1}	–	[5]
EWB	107.88 mg·g^{-1}	109.65 mg·g^{-1}	This article

Fig. 11. Regenerating efficiency of EWB.

media) for the adsorption of Cu(II) and Cr(VI). According to the statistics, EWB has the highest adsorption efficiency of any adsorbent. However, when the EWB adsorbent was used, three removal mechanisms, electrostatic attraction, ion exchange, and chelation mechanism, existed simultaneously, leading to a greater adsorption capacity used in our experiment.

3.7. Regeneration of adsorbent

Regeneration and desorption of adsorbents are crucial components of toxic metal adsorption processes because they govern the economics of water treatment technology [57]. For toxic metals recovery and effective regeneration of adsorbents, acids (such as CH_3COOH, $HCOOH$, HNO_3, H_2SO_4, and HCl), alkalis (such as K_2CO_3, KOH, Na_2CO_3, $NaHCO_3$ and NaOH), salts (such as $C_6H_5Na_3O_7$·$2H_2O$, KNO_3, NH_4NO_3, $CaCl_2$·$2H_2O$, $(NH_4)_2SO_4$, KCl and NaCl), buffer solutions (such as phosphate and bicarbonate), chelating agents and deionized water were used in various studies

[58]. In this study, deionized water and 0.1 M HCl was used for the desorption experiment. The spent EWB was added to 0.1 M HCl and was agitated for 30 min, the EWB was then recovered by filtration followed by drying in oven. The dried, cleaned EWB was then used to absorb a new batch of wastewater. EWB was cycled six times, and the percentage adsorption results of Cr(VI) and Cu(II) in each cycle are shown in Fig. 11. The statistics clearly show that the EWB can be used for adsorption up to four times in a row with little decrease in efficiency. After the fourth cycle, however, the efficiency drastically decreased, presumably as a result of a change in the EWB function. These findings were in agreement with the findings of [59,60].

4. Conclusions

Herein, we have provided a simple method for preparing EWB from eucalyptus wood waste. The prepared EWB can be severed as an efficient adsorbent to remove Cu(II) and Cr(VI) from wastewater as well as aqueous solution (>95%). The EWB possesses a larger specific surface area, which provides sufficient active adsorption sites for Cr(VI) and Cu(II). Additionally, a thorough investigation of the external factors influencing adsorption performance was conducted. The results showed that the EWB had a high removal efficiency and improved reusability. The adsorption process is well modelled by the pseudo-second-order and Langmuir models. The results of this study suggest that EWB is a promising adsorbent with the ability to successfully remove Cr(VI) and Cu(II) from aqueous solutions. As far as the reduction of wastewater is concerned, the current research proves to be a milestone in the reduction of environmental pollution. For future work, we plan to examine the adsorption efficiency of EWB for organic and inorganic pollutants.

References

[1] M. Ilyas, W. Ahmad, H. Khan, I. Ahmad, Application of composite adsorbents prepared from waste PS and PET for removal of Cr and Cu ions from wastewater, Desal. Water Treat., 171 (2019) 144–157.

[2] M. Ilyas, W. Ahmad, H. Khan, S. Yousaf, M. Yasir, A. Khan, Environmental and health impacts of industrial wastewater effluents in Pakistan: a review, Rev. Environ. Health, 34 (2019) 171–186.

[3] N.K. Srivastava, C.B. Majumder, Novel biofiltration methods for the treatment of heavy metals from industrial wastewater, J. Hazard. Mater., 151 (2008) 1–8.

[4] S. Díaz, A. Martín-González, J.C. Gutiérrez, Evaluation of heavy metal acute toxicity and bioaccumulation in soil ciliated protozoa, Environ. Int., 32 (2006) 711–717.

[5] J.H. Potgieter, S.S. Potgieter-Vermaak, P.D. Kalibantonga, Heavy metals removal from solution by palygorskite clay, Miner. Eng., 19 (2006) 463–470.

[6] R. Camarillo, A. Pérez, P. Cañizares, A. de Lucas, Removal of heavy metal ions by polymer enhanced ultrafiltration: batch process modeling and thermodynamics of complexation reactions, Desalination, 286 (2012) 193–199.

[7] S. Schiewer, S.B. Patil, Modeling the effect of pH on biosorption of heavy metals by citrus peels, J. Hazard. Mater., 157 (2008) 8–17.

[8] A.M. Al Ketife, F. Almomani, H. Znad, Sustainable removal of copper from wastewater using chemically treated bio-sorbent: characterization, mechanism and process kinetics, Environ. Technol. Innovation, 23 (2021) 101555, doi: 10.1016/j.eti.2021.101555.

[9] E.N. Mahmoud, F.Y. Fayed, K.M. Ibrahim, S. Jaafreh, Removal of cadmium, copper, and lead from water using bio-sorbent from treated olive mill solid residue, Environ. Health Insights, 15 (2021), doi: 10.1177/11786302211053176.

[10] K.Z. Elwakeel, A.A. El-Bindary, E.Y. Kouta, E. Guibal, Functionalization of polyacrylonitrile/Na-Y-zeolite composite with amidoxime groups for the sorption of Cu(II), Cd(II) and Pb(II) metal ions, Chem. Eng. J., 332 (2018) 727–736.

[11] K. Rambabu, A. Thanigaivelan, G. Bharath, N. Sivarajasekar, F. Banat, P.L. Show, Biosorption potential of *Phoenix dactylifera* coir wastes for toxic hexavalent chromium sequestration, Chemosphere, 268 (2021) 128809, doi: 10.1016/j.chemosphere.2020.128809.

[12] K.Z. Elwakeel, A.S. Al-Bogami, A.M. Elgarahy, Efficient retention of chromate from industrial wastewater onto a green magnetic polymer based on shrimp peels, J. Polym. Environ., 26 (2018) 2018–2029.

[13] A. Mittal, R. Ahmad, I. Hasan, Biosorption of Pb²⁺, Ni²⁺ and Cu²⁺ ions from aqueous solutions by L-cystein-modified montmorillonite-immobilized alginate nanocomposite, Desal. Water Treat., 57 (2016) 17790–17807.

[14] W.S. Chai, W.G. Tan, H.S.H. Munawaroh, V.K. Gupta, S.-H. Ho, P.L. Show, Multifaceted roles of microalgae in the application of wastewater biotreatment: a review, Environ. Pollut., 269 (2021) 116236, doi: 10.1016/j.envpol.2020.116236.

[15] A.A. Atia, A.M. Donia, K.Z. ELwakeel, Adsorption behaviour of non-transition metal ions on a synthetic chelating resin bearing iminoacetate functions, Sep. Purif. Technol., 43 (2005) 43–48.

[16] A. Mittal, R. Ahmad, I. Hasan, Poly(methyl methacrylate)-grafted alginate/Fe₃O₄ nanocomposite: synthesis and its application for the removal of heavy metal ions, Desal. Water Treat., 57 (2016) 19820–19833.

[17] M. Agarwa, K. Singh, Heavy metal removal from wastewater using various adsorbents: a review, J. Water Reuse Desal., 7 (2017) 387–419.

[18] A.M. Elgarahy, K.Z. Elwakeel, S.H. Mohammad, G.A. Elshoubaky, A critical review of biosorption of dyes, heavy metals and metalloids from wastewater as an efficient and green process, Cleaner Eng. Technol., 4 (2021) 100209, doi: 10.1016/j.clet.2021.100209.

[19] N.M. Alandis, W. Mekhamer, O. Aldayel, J.A. Hefne, M. Alam, Adsorptive applications of montmorillonite clay for the removal of Ag(I) and Cu(II) from aqueous medium, J. Chem., 2019 (2019) 7129014, doi: 10.1155/2019/7129014.

[20] M.R. Awual, T. Yaita, H. Shiwaku, S. Suzuki, A novel facial composite adsorbent for enhanced copper(II) detection and removal from wastewater, Chem. Eng. J., 266 (2015) 368–375.

[21] A.M. Elgarahy, K.Z. Elwakeel, A. Akhdhar, M.F. Hamza, Recent advances in greenly synthesized nanoengineered materials for water/wastewater remediation: an overview, Nanotechnol. Environ. Eng., 6 (2021) 1–24.

[22] C. Vanlalveni, S. Lallianrawna, A. Biswas, M. Selvaraj, B. Changmai, S.L. Rokhum, Green synthesis of silver nanoparticles using plant extracts and their antimicrobial activities: a review of recent literature, RSC Adv., 11 (2021) 2804–2837.

[23] R. Awual, M. Hasan, A ligand based innovative composite material for selective lead(II) capturing from wastewater, J. Mol. Liq., 294 (2019) 111679, doi: 10.1016/j.molliq.2019.111679.

[24] K.Z. Elwakeel, A.M. Elgarahy, Z.A. Khan, M.S. Almughamisi, A.S. Al-Bogami, Perspectives regarding metal/mineral-incorporating materials for water purification: with special focus on Cr(VI) removal, Mater. Adv., 1 (2020) 1546–1574.

[25] A. Mittal, R. Ahmad, I. Hasan, Iron oxide-impregnated dextrin nanocomposite: synthesis and its application for the biosorption of Cr(VI) ions from aqueous solution, Desal. Water Treat., 57 (2016) 15133–15145.

[26] M.R. Awual, Ring size dependent crown ether based mesoporous adsorbent for high cesium adsorption from wastewater, Chem. Eng. J., 303 (2016) 539–546.

[27] A. Benettayeb, A. Morsli, K.Z. Elwakeel, M.F. Hamza, E. Guibal, Recovery of heavy metal ions using magnetic glycine-modified chitosan—application to aqueous solutions and tailing leachate, Appl. Sci., 11 (2021) 8377, doi: 10.3390/app11188377.

[28] J. Mittal, R. Ahmad, A. Mariyam, V.K. Gupta, A. Mittal, Expeditious and enhanced sequestration of heavy metal ions from aqueous environment by papaya peel carbon: a green and low-cost adsorbent, Desal. Water Treat., 210 (2021) 365–376.

[29] M.R. Awual, T. Yaita, S. Suzuki, H. Shiwaku, Ultimate selenium(IV) monitoring and removal from water using a new class of organic ligand based composite adsorbent, J. Hazard. Mater., 291 (2015) 111–119.

[30] K.Z. Elwakeel, A. Shahat, A.S. Al-Bogami, B. Wijesiri, A. Goonetilleke, The synergistic effect of ultrasound power and magnetite incorporation on the sorption/desorption behavior of Cr(VI) and As(V) oxoanions in an aqueous system, J. Colloid Interface Sci., 569 (2020) 76–88.

[31] R. Ahmad, I. Hasan, A. Mittal, Adsorption of Cr(VI) and Cd(II) on chitosan grafted polyaniline-OMMT nanocomposite: isotherms, kinetics and thermodynamics studies, Desal. Water Treat., 58 (2017) 144–153.

[32] M.R. Awual, T. Yaita, T. Kobayashi, H. Shiwaku, S. Suzuki, Improving cesium removal to clean-up the contaminated water using modified conjugate material, J. Environ. Chem. Eng., 8 (2020) 103684, doi: 10.1016/j.jece.2020.103684.

[33] M.S. Almughamisi, Z.A. Khan, W. Alshitari, K.Z. Elwakeel, Recovery of chromium(VI) oxyanions from aqueous solution using Cu(OH)₂ and CuO embedded chitosan adsorbents, J. Polym. Environ., 28 (2020) 47–60.

[34] H. Daraei, A. Mittal, Investigation of adsorption performance of activated carbon prepared from waste tire for the removal of methylene blue dye from wastewater, Desal. Water Treat., 90 (2017) 294–298.

[35] M.R. Awual, Assessing of lead(III) capturing from contaminated wastewater using ligand doped conjugate adsorbent, Chem. Eng. J., 289 (2016) 65–73.

[36] K.Z. Elwakeel, E. Guibal, Potential use of magnetic glycidyl methacrylate resin as a mercury sorbent: from basic study to the application to wastewater treatment, J. Environ. Chem. Eng., 4 (2016) 3632–3645.

[37] S. Soni, P.K. Bajpai, D. Bharti, J. Mittal, C. Arora, Removal of crystal violet from aqueous solution using iron-based metal organic framework, Desal. Water Treat., 205 (2020) 386–399.

[38] M.R. Awual, T. Yaita, H. Shiwaku, Design a novel optical adsorbent for simultaneous ultra-trace cerium(III) detection, sorption and recovery, Chem. Eng. J., 228 (2013) 327–335.

[39] M.R. Awual, Solid phase sensitive palladium(II) ions detection and recovery using ligand based efficient conjugate nanomaterials, Chem. Eng. J., 300 (2016) 264–272.

[40] M.R. Awual, A novel facial composite adsorbent for enhanced copper(II) detection and removal from wastewater, Chem. Eng. J., 266 (2015) 368–375.

[41] M.R. Awual, A facile composite material for enhanced cadmium(II) ion capturing from wastewater, J. Environ. Chem. Eng., 7 (2019) 103378, doi: 10.1016/j.jece.2019.103378.

[42] N.B.M. Zain, N.J.M. Salleh, N.F. Hisamuddin, S. Hashim, N.H. Abdullah, Adsorption of phosphorus using cockle shell waste, Ind. Domest. Waste Manage., 2 (2022) 30–38.

[43] M. Salman, M. Demir, K.H. Tang, L.T. Cao, S. Bunrith, T.W. Chen, N.M. Darwish, B.M. AlMunqedhi, T. Hadibarata, Removal of cresol red by adsorption using wastepaper, Ind. Domest. Waste Manage., 2 (2022) 1–8.

[44] Z. Ishak, D. Kumar, Adsorption of methylene blue and Reactive black 5 by activated carbon derived from tamarind seeds, Trop. Aquat. Soil Pollut., 2 (2022) 1–2.

[45] Z.H. Ho, L.A. Adnan, Phenol removal from aqueous solution by adsorption technique using coconut shell activated carbon, Trop. Aquat. Soil Pollut., 1 (2021) 98–107.

[46] M. Ahmad, A.U. Rajapaksha, J.E. Lim, M. Zhang, N. Bolan, D. Mohan, M. Vithanage, S.S. Lee, Y.S. Ok, Biochar as a sorbent for contaminant management in soil and water: a review, Chemosphere, 99 (2014) 19–33.

[47] A. Awoyemi, Understanding the Adsorption of Polycyclic Aromatic Hydrocarbons from Aqueous Phase onto Activated Carbon, Doctoral Dissertation, 2011.

[48] S. Athapaththu, A Comprehensive Study of Cd(II) Removal From Aqueous Solution Via Adsorption and Solar Photocatalysis, Electronic Thesis and Dissertation Repository, vol. 19, 2013, p. 1783.

[49] K.G. Bhattacharyya, S.S Gupta, Pb(II) uptake by kaolinite and montmorillonite in aqueous medium: influence of acid activation of the clays, Colloids Surf., A, 277 (2006) 191–200.

[50] M. Hamidpour, M. Kalbasi, M. Afyuni, H. Shariatmadari, G. Furrer, Sorption of lead on Iranian bentonite and zeolite: kinetics and isotherms, Environ. Earth Sci., 62 (2011) 559–568.

[51] M.R. Shrestha, I. Varga, J. Bajtai, M. Varga, Design of surface functionalization of waste material originated charcoals by an optimized chemical carbonization for the purpose of heavy metal removal from industrial wastewater, Microchem. J., 108 (2013) 224–232.

[52] Y. Kong, J. Wei, Z. Wang, T. Sun, C. Yao, Z. Chen, Heavy metals removal from solution by polyaniline/palygorskite composite, J. Appl. Polym. Sci., 122 (2011) 2054–2059.

[53] M. Kobya, E. Demirbas, E. Senturk, M. Ince, Adsorption of heavy metal ions from aqueous solutions by activated carbon prepared from apricot stone, Bioresour. Technol., 96 (2005) 1518–1521.

[54] A. Sarı, M. Tuzen, D. Cıtak, M. Soylak, Adsorption characteristics of Cu(II) and Pb(II) onto expanded perlite from aqueous solution, J. Hazard. Mater., 148 (2007) 387–394.

[55] H. Chen, Y. Zhao, A. Wang, Removal of Cu(II) from aqueous solution by adsorption onto acid-activated palygorskite, J. Hazard. Mater., 149 (2007) 346–354.

[56] S.M. Xu, J. Wei, S. Feng, J.D. Wang, X.S. Li, A study in the adsorption behaviors of Cr(VI) on crosslinked cationic starches, J. Polym. Res., 11 (2004) 211–215.

[57] I. Ali, New generation adsorbents for water treatment, Chem. Rev., 112 (2012) 5073–5091.

[58] S. Lata, P.K. Singh, S.R. Samadder, Regeneration of adsorbents and recovery of heavy metals: a review, Int. J. Environ. Sci. Technol., 12 (2015) 1461–1478.

[59] T. Motsi, Remediation of Acid Mine Drainage Using Natural Zeolite, School of Chemical Engineering, The University of Birmingham, United Kingdom, 2010.

[60] T. Motsi, N.A. Rowson, M.J.H. Simmons, Adsorption of heavy metals from acid mine drainage by natural zeolite, Int. J. Miner. Process., 92 (2009) 42–48.